Hindawi Publishing Corporation
Journal of Sensors
Volume 2016, Article ID 8296936, 5 pages
http://dx.doi.org/10.1155/2016/8296936

Research Article

Highly Responsive UV Light Sensors Using Mg-Doped ZnO Nanoparticles

Mirza Shirjeel Alam,[1] Umair Manzoor,[1,2] Mohammad Mujahid,[3] and Arshad S. Bhatti[1]

[1]*Center for Micro and Nano Devices (CMND), Department of Physics, COMSATS Institute of Information Technology, Islamabad 44000, Pakistan*
[2]*Alamoudi Water Research Chair, King Saud University, P.O. Box 2460, Riyadh 11451, Saudi Arabia*
[3]*School of Chemical & Materials Engineering (SCME), National University of Sciences & Technology (NUST), Sector H-12, Islamabad 44000, Pakistan*

Correspondence should be addressed to Umair Manzoor; umanzoor@ksu.edu.sa

Received 30 December 2015; Revised 4 February 2016; Accepted 28 February 2016

Academic Editor: Christos Riziotis

Different concentrations of Mg-doped ZnO nanoparticles (NPs) were synthesized by coprecipitation technique at 60°C. XRD data are used to study phase purity and crystal structure in different doping concentrations. The results indicated that increasing the doping from 0~7.5 wt.% caused a subsequent increase in FWHM in XRD and an associated systematic shift towards higher wavelength in the optical properties. Finally, the sensing of UV light is tested by observing the response of nanoparticles by exposing them to UV light and measuring the resistance in presence and absence of UV light.

1. Introduction

Oxides are now a smart choice and basis of advanced and multifunctional devices [1]. Device fabrication and synthesis using oxides semiconductor have become more important recently because the physical properties are size dependent and can be tuned. Among oxide semiconductor family, ZnO is a wide bandgap material (3.37 eV at room temperature) with large exciton binding energy (60 meV) and strong photocatalytic, optical, and piezoelectric properties. They are used in solar cells, photocatalysis and antibacterial active material [2], gas sensors [3], and UV (Ultraviolet) light emitting/detecting devices [4]. ZnO is also an integral part of green luminescence phosphor in fluorescent devices [5].

UV sensors are widely used in different applications, such as pollution monitoring, flame sensing, early missile plume detection, and other advanced military applications [6]. Different types of Si-based photodetectors are already available in the market and are very sensitive with low noise and quick response [5]. However, applications are limited as some need ultrahigh vacuum or high voltage supply (i.e., in photomultipliers) or time dependent degradation and lower efficiency [7]. To overcome these disadvantages, new materials such as diamond, SiC, oxide semiconductors, and nitrides are a focus of research because of their intrinsic visible-blindness. Also, chemical and thermal stability at operating conditions are far better than the conventional materials. Moreover, their optical properties are slightly temperature dependent [8, 9]. One of the possible materials which fulfills most of these requirements is ZnO. Therefore, it has been studied extensively recently to further explore its potential applications in electronics and optoelectronics [10]. Furthermore, different doping in ZnO (i.e., Mg) can adjust bandgap to make UV photodetectors in different UV regime [11, 12]. Despite a great deal of research on ZnO UV detector, most of the research concentrated on the improvements of the micromask electrodes, in order to enhance the performance of the ZnO photoconductive detectors [11]. ZnO sensing mechanism can be linked with surface reactions. Hence, grain size, defects, and oxygen adsorption are important parameters for controlling sensing response [3].

In the present study, systematic Mg doping (0~7.5 wt.%) in ZnO NPs was achieved and is analysed by XRD, FTIR, and

Table 1: Experimental details and chemical quantities used for the synthesis.

#	% age doping	$Zn(CH_3COO)_2$ (g)	$Mg(CH_3COO)_2$ (g)	KOH (g)	Ethanol (mL)	Other constants (same for all experiments)
1	0%	1.004	—	0.990	80	Temperature: 60°C Constant stirring: 2.5 hours Centrifuged to separate ZnO NPs Repeatedly washed with distilled water and ethanol, at 60°C
2	2.5%	1.009	0.020	1.008	80	
3	5.0%	1.007	0.041	0.960	80	
4	7.5%	1.003	0.078	0.962	80	

UV-Vis spectroscopy. Optical properties were tuned by Mg doping. UV sensing properties are also demonstrated. The main focus of the study was the fast response time of Mg-doped ZnO NPs as active sensor material.

2. Experimental Section

Zinc acetate dihydrate ($Zn(CH_3COO)_2$, Sigma-Aldrich) and 1 mL of water (distilled) were put into a flask containing 80 mL methanol. They were mixed at 60°C. In a second beaker, potassium hydroxide (KOH, Sigma-Aldrich) was dissolved in 23 mL of methanol. The solution was then slowly added into the flasks containing zinc acetate. This mixture was then stirred for 2.5 hours. The transparent solution became opaque because of slow addition of KOH which, again, slowly transformed into a clear solution. ZnO powder was separated from the solvent by centrifuge and repeatedly washed in distilled water and ethanol. The powder was dried in convection oven at 60°C. For doping, magnesium acetate dihydrate ($Mg(CH_3COO)_2$ Sigma-Aldrich) was added in appropriate quantities. The experimental details and quantities are shown in Table 1.

The morphology was determined using transmission electron microscope (TEM, JEOL). The phase analysis was done using X-ray diffraction technique (JDX-11, Japan). Diffuse reflectance spectroscopy (DRS) of NPs was done by using a Lamda-950 Perkin-Elmer. Thick film sensors were made by doctor blading (same area and thickness for all sensors) and resistance was measured using multimeter (Keithly 2000 multimeter).

3. Results and Discussion

Figure 1 illustrates XRD spectrum of different NPs prepared by the coprecipitation method. All major diffraction peaks can be assigned to diffraction from different ZnO planes, respectively (JCPDS card # 780-0075). There is a weak peak at about 27° in 5% Mg-doped sample, which can be due to $Zn(CH_3COO)_2$ as a result of unwanted residue left in the sample [14]. This revealed that the resultant NPs were phase-pure ZnO (no MgO peaks) with a hexagonal structure. MgO has rock-salt structure and ZnO has hexagonal structure. Therefore, phase separation can occur at higher concentrations. The XRD spectra clearly suggest that there is no phase separation. Zn and Mg ions have similar ionic radii (0.60 and 0.57 Å) and it is expected that Mg ions are substituted for Zn. The systematic peak shift and broader FWHM with consistent increase in Mg doping is are indication of doping, suggesting a higher defect concentration and decreased quality of crystal

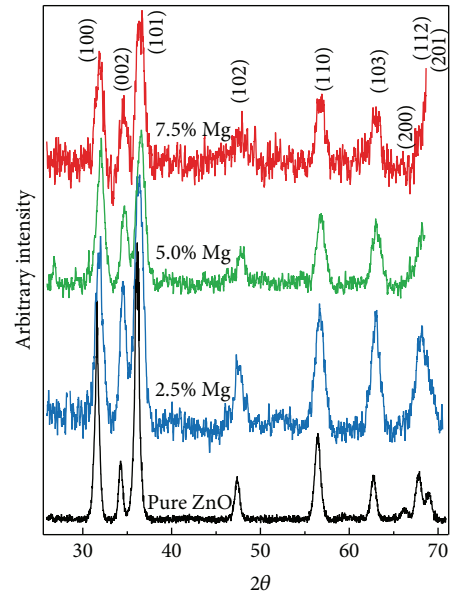

Figure 1: XRD spectra of different levels of Mg doping in ZnO NPs. The results clearly show that all the major peaks correspond to ZnO. There is a systematic broadening of FWHM with an increase in doping concentration.

with increase in Mg doping concentration. Also, there is a clear systematic (101) peak (highest intensity) shift towards higher 2 theta value. This again is another indication of change in "*d*" spacing with increase in the doping concentration. Figure S1 (at Supplementary Material available online at http://dx.doi.org/10.1155/2016/8296936) shows a TEM image of pure ZnO NPs and clearly suggests that the average particle size is less than 10 nm. Also, there are 2 minor peaks ((200) and (201)) which disappear after doping. One of the possible reasons can be that these peaks shift because of the Mg-induced strain and merge into the broader (112) peak. This peak broadening can be clearly observed if XRD spectra of pure ZnO and 2.5% Mg samples are compared. Also, the morphology is dependent on doping and previous researchers suggested that grain size increases with increase in doping concentration.

Figure 2 represents the FTIR results in the range of 4000 cm^{-1} to 500 cm^{-1}. 3550 cm^{-1} to 3250 cm^{-1} band is typically the stretching vibration mode of OH^- group. Also, 1650 cm^{-1} band is the OH^- fundamental stretching mode. These bands are very typical signals of H_2O present on the sample surface. Zn-O stretching mode is located at 560 cm^{-1}

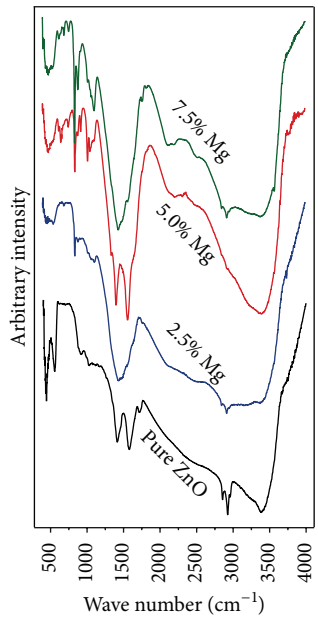

FIGURE 2: FTIR results of different levels of Mg doping in ZnO NPs. A clear change of ZnO stretching modes with increase in Mg doping (around 500 cm^{-1}) suggests that Zn ions are replaced by Mg ions.

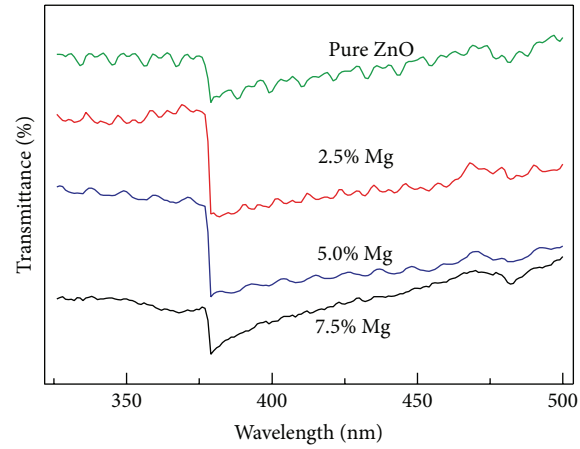

FIGURE 3: UV-Vis spectroscopy of samples with pure and different concentrations of Mg-doped ZnO. The results give a clear indication of direct band emission, in UV region, for all the samples. There is also a systematic shift towards higher wavelength for UV emission. Minor peaks around 475 nm can be the defect related deep-level emission peaks [13].

to 600 cm^{-1} [15]. There is a slight systematic peak shift of Zn-O band which can be an indirect evidence of increasing Mg content in the lattice. Mg-O stretching vibrations can also be clearly observed in the region of 1400 cm^{-1} to 1450 cm^{-1}. FTIR results give a clear indication that Mg was successfully doped in ZnO lattice [15, 16].

Bandgap of ZnO NPs can be effectively tuned by doping Mg^{2+}. The bandgap of ZnO and MgO is 3.37 eV and 7.7 eV, respectively, and it can be increased by Mg doping [12]. The UV-visible spectroscopy results are shown in Figure 3. The bandgap of all the samples can be estimated by converting wave length into the energy using the following equation:

$$E = hc \setminus \lambda, \tag{1}$$

where "E" is energy, "h" is Plank's constant, "c" is velocity of light, and "λ" is the wave length. A systematic blue shift in the main UV peak can be clearly observed with the increase in the Mg doping and the bandgap ranges from 3.24 eV for pure ZnO to 3.33 eV for 7.5% Mg samples. Our results are in accordance with the previous studies and clearly show that bandgap can be tuned by carefully controlling Mg doping [17, 18]. One of the possible explanations of this blue shift is the Burstein-Moss effect. Fermi level of n type ZnO is inside the conduction band. With Mg doping, the conduction bands are filled. This in turn shifts the absorption edge to the higher energy [19].

Photoconductive response time is important for a UV sensor. Electron-hole pairs are generated on UV exposure. These holes are then combined with trapped oxygen ions, commonly known as surface electron-hole recombination. This effect is shown in [20]

$$h^{+} + O_2^{-}\,(\text{ad}) \longrightarrow O_2\,(\text{gas}) \tag{2}$$

Unpaired electrons are freely available and enhance the photocurrent. Figure 4 is the sensing results of Mg-doped ZnO NPs done at room temperature. The On-Off switch time was very small (in seconds) and one of the main focuses of this experiment was to investigate the response time and change in resistance with Mg doping. The sensitivity (ratio of resistance in the dark and in the presence of UV light) is 1.060, 1.062, 1.088, and 1.054 for 0%, 2.5%, 5.0%, and 7.5%, respectively. The enhanced response of Mg-doped ZnO NPs can be attributed to unpaired electrons added to the photocurrent [21, 22]. In ZnO, oxygen vacancies act as electron donors. Surface defects and charged species increase after the Mg doping, thus more reaction and surface recombination results in faster response time. Also, NPs are a good choice for obtaining fast response of the devices due to an enhanced surface to volume ratio [23]. However, the decrease in sensitivity after 7.5% Mg can be attributed to severe damage in the crystal lattice. Previous researchers have also suggested that the Mg-doped ZnO (and $Zn_{1-x}Mg_xO$) having potential photodetectors with different detective wavelengths have strong potential for being the sensor active material. However, there is a wide miscibility gap and large lattice mismatch in the ZnO-MgO binary system. This is mainly because of the difference in crystal structure. Therefore, defect density increases and crystal quality is low. Also phase segregation can occur. This has become the major issue for synthesis. Also, finding new materials with faster adsorption and disadsorption characteristics is the main issue which is attracting the attention of researchers in this field [24–28]. It was also suggested that, usually with doping, the bandgap is shifted to the lower energy region, which enhances the absorption spectrum of doped ZnO NPs [29]. These are the main issues which are attracting the attention of researchers in this field.

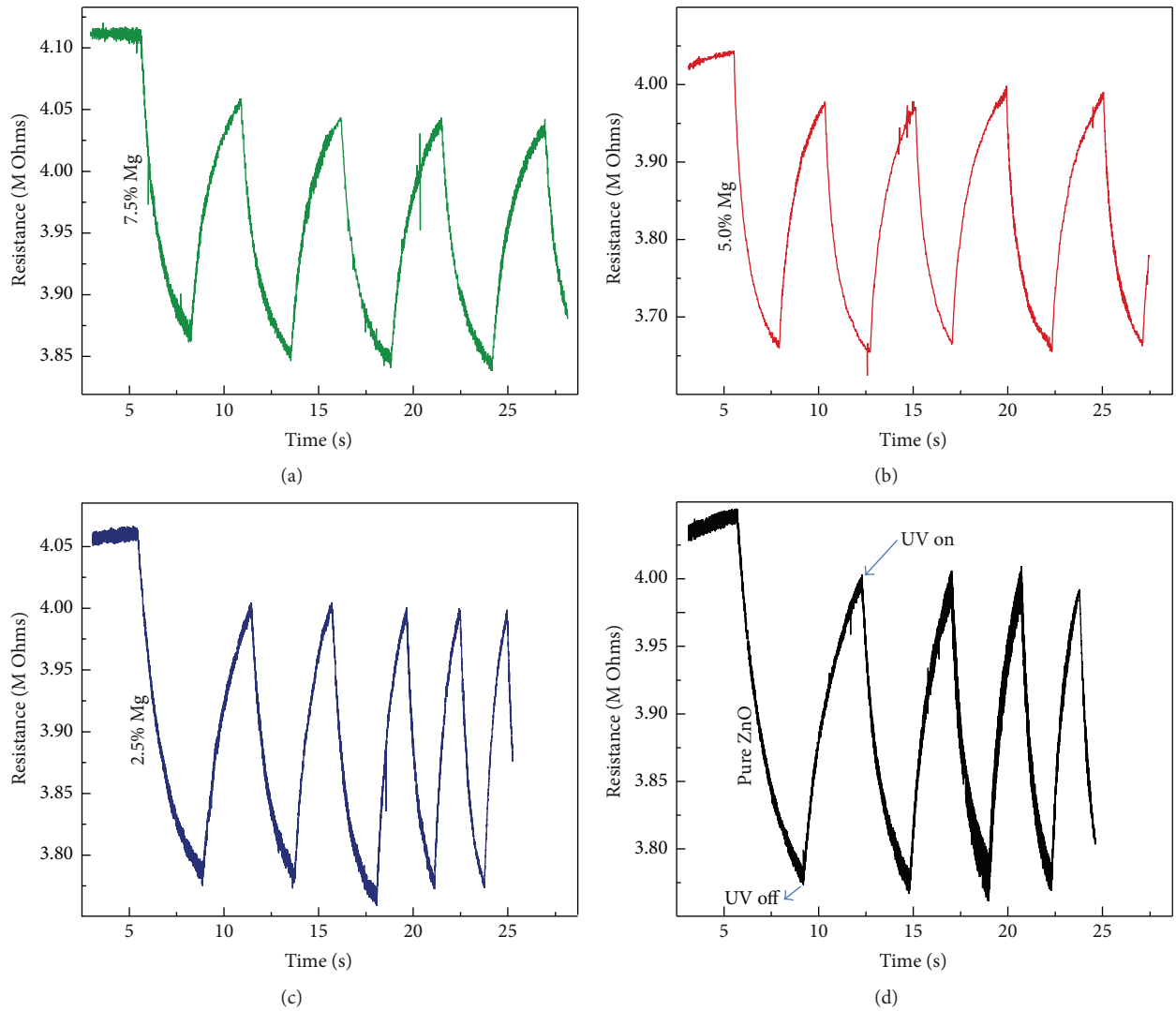

Figure 4: Room temperature UV sensor results of different samples with Mg doping (a) 7.5% (b), 5.0%, (c) 2.5%, and (d) pure ZnO. The results clearly suggest good sensitivity for all the doped and undoped samples.

XRD, UV-Vis spectroscopy, and optical sensor results are in perfect agreement with each other. There is a systematic peak shift in XRD and UV-Vis results with increase in Mg doping. XRD peak shift also indicates changes in *"d spacing."* The UV sensing properties of Mg-doped ZnO NPs show fast switching behavior due to adsorbed oxygen.

4. Conclusions

Pure and Mg-doped ZnO NPs were prepared by coprecipitation method at 60°C. XRD spectra show a regular peak shift towards higher angle with a wider FWHM. FTIR results give a clear indication of the presence of Mg atoms in the lattice by showing Zn-O band shift towards the high energy and also the appearance of Mg-O vibration peak. One of the motives of Mg doping is to tune the optical properties of ZnO NPs. The bandgap of NPs was directly related to the concentration of Mg atoms in particles. The sensing results showed very fast response towards UV light for all the samples.

Competing Interests

The authors declare that there is no conflict of interests regarding the publication of this paper.

Authors' Contributions

Mirza Shirjeel Alam, Umair Manzoor, Mohammad Mujahid, and Arshad S. Bhatti contributed equally to this work.

Acknowledgments

This project was funded by the National Plan for Science, Technology and Innovation (MAARIFAH), King Abdulaziz

City for Science and Technology, Kingdom of Saudi Arabia, Award no. 2623.

References

[1] Z. R. Dai, Z. W. Pan, and Z. L. Wang, "Novel nanostructures of functional oxides synthesized by thermal evaporation," *Advanced Functional Materials*, vol. 13, no. 1, pp. 9–24, 2003.

[2] K. Rekha, M. Nirmala, M. G. Nair, and A. Anukaliani, "Structural, optical, photocatalytic and antibacterial activity of zinc oxide and manganese doped zinc oxide nanoparticles," *Physica B: Condensed Matter*, vol. 405, no. 15, pp. 3180–3185, 2010.

[3] M. Amin, U. Manzoor, M. Islam, A. S. Bhatti, and N. A. Shah, "Synthesis of ZnO nanostructures for low temperature CO and UV sensing," *Sensors*, vol. 12, no. 10, pp. 13842–13851, 2012.

[4] L. Peng, L. Hu, and X. Fang, "Low-dimensional nanostructure ultraviolet photodetectors," *Advanced Materials*, vol. 25, no. 37, pp. 5321–5328, 2013.

[5] H.-M. Xiong, D. G. Shchukin, H. Möhwald, Y. Xu, and Y.-Y. Xia, "Sonochemical synthesis of highly luminescent zinc oxide nanoparticles doped with magnesium(II)," *Angewandte Chemie—International Edition*, vol. 48, no. 15, pp. 2727–2731, 2009.

[6] W. Bunjongpru, P. Panprom, S. Porntheeraphat et al., "UV-enhanced photodetector with nanocrystalline-TiO_2 thin film via CMOS compatible process," in *Proceedings of the IEEE Nanotechnology Materials and Devices Conference (NMDC '11)*, pp. 364–367, IEEE, Jeju, South Korea, October 2011.

[7] J. Cao, J. Wang, B. Fang, X. Chang, M. Zheng, and H. Wang, "Microwave-assisted synthesis of flower-like ZnO nanosheet aggregates in a room-temperature ionic liquid," *Chemistry Letters*, vol. 33, no. 10, pp. 1332–1333, 2004.

[8] U. Manzoor and D. K. Kim, "Size control of ZnO nanostructures formed in different temperature zones by varying Ar flow rate with tunable optical properties," *Physica E: Low-Dimensional Systems and Nanostructures*, vol. 41, no. 3, pp. 500–505, 2009.

[9] W. Q. Peng, S. C. Qu, G. W. Cong, and Z. G. Wang, "Synthesis and temperature-dependent near-band-edge emission of chain-like Mg-doped ZnO nanoparticles," *Applied Physics Letters*, vol. 88, no. 10, Article ID 101902, 2006.

[10] U. Manzoor, M. Islam, L. Tabassam, and S. U. Rahman, "Quantum confinement effect in ZnO nanoparticles synthesized by co-precipitate method," *Physica E: Low-Dimensional Systems and Nanostructures*, vol. 41, no. 9, pp. 1669–1672, 2009.

[11] X. L. Zhang, K. S. Hui, and K. N. Hui, "High photo-responsivity ZnO UV detectors fabricated by RF reactive sputtering," *Materials Research Bulletin*, vol. 48, no. 2, pp. 305–309, 2013.

[12] Y. Jin, Y. Ren, M. Cao, and Z. Ye, "Doped colloidal ZnO nanocrystals," *Journal of Nanomaterials*, vol. 2012, Article ID 985326, 8 pages, 2012.

[13] E. Burstein, "Anomalous optical absorption limit in InSb," *Physical Review*, vol. 93, no. 3, pp. 632–633, 1954.

[14] F. K. Shan, B. I. Kim, G. X. Liu et al., "Blueshift of near band edge emission in Mg doped ZnO thin films and aging," *Journal of Applied Physics*, vol. 95, no. 9, pp. 4772–4776, 2004.

[15] D. L. Golić, G. Branković, M. P. Nešić et al., "Structural characterization of self-assembled ZnO nanoparticles obtained by the sol–gel method from $Zn(CH_3COO)_2.2H_2O$," *Nanotechnology*, vol. 22, no. 39, Article ID 395603, 2011.

[16] G. H. Ning, X.-P. Zhao, and J. Li, "Structure and optical properties of $Mg_xZn_{1-x}O$ nanoparticles prepared by sol-gel method," *Optical Materials*, vol. 27, pp. 1–5, 2004.

[17] R. Wahab, S. G. Ansari, Y. S. Kim et al., "Low temperature solution synthesis and characterization of ZnO nano-flowers," *Materials Research Bulletin*, vol. 42, no. 9, pp. 1640–1648, 2007.

[18] A. Ohtomo, K. Tamura, M. Kawasaki et al., "Room-temperature stimulated emission of excitons in ZnO/(Mg, Zn)O superlattices," *Applied Physics Letters*, vol. 77, no. 14, pp. 2204–2206, 2000.

[19] H.-C. Hsu, C.-Y. Wu, H.-M. Cheng, and W.-F. Hsieh, "Band gap engineering and stimulated emission of ZnMgO nanowires," *Applied Physics Letters*, vol. 89, Article ID 013101, 2006.

[20] U. Manzoor and D. K. Kim, "Synthesis and enhancement of ultraviolet emission by post-thermal treatment of unique zinc oxide comb-shaped dendritic nanostructures," *Scripta Materialia*, vol. 54, no. 5, pp. 807–811, 2006.

[21] K. ul Hasan, N. H. Alvi, J. Lu, O. Nur, and M. Willander, "Single nanowire-based UV photodetectors for fast switching," *Nanoscale Research Letters*, vol. 6, article 348, 2011.

[22] H. Kind, H. Yan, B. Messer, M. Law, and P. Yang, "Nanowire ultraviolet photodetectors and optical switches," *Advanced Materials*, vol. 14, no. 2, pp. 158–160, 2002.

[23] C. Soci, A. Zhang, B. Xiang et al., "ZnO nanowire UV photodetectors with high internal gain," *Nano Letters*, vol. 7, no. 4, pp. 1003–1009, 2007.

[24] M.-W. Chen, C.-Y. Chen, D.-H. Lien, Y. Ding, and J.-H. He, "Photoconductive enhancement of single ZnO nanowire through localized Schottky effects," *Optics Express*, vol. 18, no. 14, pp. 14836–14841, 2010.

[25] R. Afrin, J. Khaliq, M. Islam, I. H. Gul, A. S. Bhatti, and U. Manzoor, "Synthesis of multiwalled carbon nanotube-based infrared radiation detector," *Sensors and Actuators A: Physical*, vol. 187, pp. 73–78, 2012.

[26] H. Liu, Z. Zhang, L. Hu et al., "New UV-A photodetector based on individual potassium niobate nanowires with high performance," *Advanced Optical Materials*, vol. 2, no. 8, pp. 771–778, 2014.

[27] N. Naderi and M. R. Hashim, "Visible-blind ultraviolet photodetectors on porous silicon carbide substrates," *Materials Research Bulletin*, vol. 48, no. 6, pp. 2406–2408, 2013.

[28] X. Fang, L. Hu, K. Huo et al., "New ultraviolet photodetector based on individual Nb_2O_5 nanobelts," *Advanced Functional Materials*, vol. 21, no. 20, pp. 3907–3915, 2011.

[29] S. Y. Bae, C. W. Na, J. H. Kang, and J. Park, "Comparative structure and optical properties of Ga-, In-, and Sn-doped ZnO nanowires synthesized via thermal evaporation," *The Journal of Physical Chemistry B*, vol. 109, no. 7, pp. 2526–2531, 2005.